

Research Paper

A Novel BESO Methodology for Topology Optimization of Reinforced Concrete Structures: A Two-loop Approach

Julian Alves Borges¹, Rodrigo Reis Amaral², Liércio André Isoldi³,
Walter Jesus Paucar Casas⁴, Herbert Martins Gomes⁵

¹ Graduate Program in Civil Engineering, Federal University of Rio Grande do Sul,
Av. Osvaldo Aranha, 99, 3° Andar, 90035-190, Porto Alegre, RS, Brazil, Email: jlnab@hotmail.com

² Graduate Program in Mechanical Engineering, Federal University of Rio Grande do Sul,
Av. Sarmento Leite, 425, Sala 202, 2° Andar, 90050-170, Porto Alegre, RS, Brazil, Email: rodrigo_amaral_23@hotmail.com

³ Graduate Program in Computational Modeling, Federal University of Rio Grande (FURG),
School of Engineering, km 8 Itália Avenue, Rio Grande, 96201-900, Brazil, Email: liercioisoldi@furg.br

⁴ Graduate Program in Mechanical Engineering, Federal University of Rio Grande do Sul,
Av. Sarmento Leite, 425, Sala 202, 2° Andar, 90050-170, Porto Alegre, RS, Brazil, Email: walter.paucar.casas@ufrgs.br

⁵ Graduate Program in Mechanical Engineering, Federal University of Rio Grande do Sul,
Av. Sarmento Leite, 425, Sala 202, 2° Andar, 90050-170, Porto Alegre, RS, Brazil, Email: herbert@mecanica.ufrgs.br

Received August 23 2022; Revised October 27 2022; Accepted for publication October 27 2022.
Corresponding author: R.R. Amaral (rodrigo_amaral_23@hotmail.com)
© 2022 Published by Shahid Chamran University of Ahvaz

Abstract. A new topology optimization methodology for reinforced concrete structures is proposed. The structures are optimized in two iterative loops, where different sensitivity criteria are used to determine the regions to be topologically optimized. For the first loop, the compliance criterion is used to determine the higher compliance elements and, consequently, remove the concrete from the computational domain. In the next loop, only failed concrete regions (Ottosen failure surface) are replaced by reinforcement, ensuring that complies with the von Mises criterion. In the end, the sizing of the reinforcements is obtained based on the principal forces in the steel regions. Results regarding the mechanical behavior, cost, volume, and mass of the optimized structures are presented in this study. A case study indicated that the proposed methodology can lead to volume, mass, and cost reductions of 20%, 21.5%, and 56%, respectively.

Keywords: Topology optimization; Reinforced concrete; BESO; Ottosen's failure surface.

1. Introduction

The design of Reinforced Concrete (RC) structures is prone to be improved by removing the underused material as well as by optimizing the geometric cross sections of the members. Some structural member types, such as deep beams with or without openings (Liang et al. [1], Nagaravan [2], and Xia et al. [3]), corbels (Lanes et al. [4], Xia et al. [5], and Cedrim et al. [6]), beam-column connections (Lee et al. [7]), pile-caps, footings (Shobeiri and Ahmadi-Nedushan [8] and Dey and Karthik [9]) and bridges (Almeida et al. [10]), just to name a few, deserve special attention due to discontinuous regions where the load path and stress/strain field are complex. Anyway, such regions still may be optimized to use the strength of the materials in the best way. This may result in material savings that, in the end, represent a less harmful carbon footprint for many members.

In the structural design, the Strut-and-Tie Model (STM) is used for sizing and detailing discontinuous structural regions of RC. In the most basic hypothesis, STM assumes an idealized truss for the load path, which may vary in shape depending on the designer's expertise. The idealized truss is used to obtain loads at the member level and to design the final detailed structure (El-Metwally and Chen [11], Goodchild et al. [12], Reineck [13], and Wight [14]). Some of these choices may work better than others. In this way, any approach that makes this choice less subjective and dependent on design experience is welcome.

Structural optimization seeks to achieve the best performance of a structure satisfying some constraints (such as volume reduction) while maintaining structural functionality and safety. Conceptually, structural optimization is divided into three major approaches: size, shape and Topology Optimization (TO). Size optimization consists in finding the ideal design by changing specific dimensions of a structure, e.g., cross-sectional thickness. Shape optimization is mainly carried out in continuous structures, for instance, by modifying their preexisting physical limits, without inserting new openings. On the other hand, TO, consists of finding the ideal design by determining the best regions to allocate or remove material in a previously defined design domain (Bendsøe and Sigmund [15]). Several TO algorithms are reported in the literature such as SIMP (Solid Isotropic with Material Penalization) [15], ETO (Evolutionary Topology Optimization) (Da et al. [16]), SEMDOT (Smooth-Edged Material Distribution for Optimizing Topology



Algorithm) (Fu et al. [17]), FPTO (Proportional Topology optimization) (Biyikli and To [18]), BESO (Bi-direction Evolutionary Structural Optimization) (Huang and Xie [19]), Level-set (Sethian and Wiegmann [20]), just to name a few. This paper will focus on the BESO implementation (regardless of the suitability of other methods), due to the easy implementation and fast analysis. Besides, not requiring explicitly gradients of objective functions is a major advantage of the BESO method compared to SIMP.

Most approaches found in the literature are using TO as a tool to define the idealized truss of the STM. Differently from those approaches, this paper is focused on proposing a novel methodology to define a high stiffer structure as well as the best positioning for the steel rebars assuring all material strength constraints are met. To do so, a new methodology to design the reinforcement of topologically optimized structures of concrete is presented. The main contribution of this work is to demonstrate the feasibility of designing RC structures with a relatively smaller amount of material. Comparisons of strength and stiffness are performed between the proposed optimized structure with structures sized and detailed based on Standards according to the well-known STM. For this, an algorithm with two iterative loops was developed in MATLAB software. For the first loop, elements with lower strain energy (compliance) are removed from the computational domain, thus forming voids in the structure. At this stage, there will only be finite elements classified as voids or concrete elements. Once the optimized topology has been obtained in the first loop, that is, the volumetric fraction stipulated by the designer has been reached; there will be the beginning of the second iterative loop. In this 2nd step of the optimization process, the addition of steel occurs in the regions of concrete that are showing structural failure, as well as the verification of the concrete and steel based on the Ottosen and von Mises criteria, respectively. The structure is considered safe when both failure criteria are met and it is assumed that at this stage the materials are still in the linear-elastic regime. Moreover, once you have the RC structure optimized, the reinforcement sizing and detailing step takes place. In this work, it is presented an evaluation of the TO parameters through a parametric analysis performed on a deep beam, and, in a second example, an analysis is performed regarding the mechanical behavior, cost, volume, and mass.

2. Literature Review

The search for structural optimization based on safety and economical designs dates back to Michell [21]. In this study, it was demonstrated the feasibility of the design of optimized structures disposing the material in a truss-like pattern. Here, the members are only subjected to tensile and compressive loads, which results in the optimum use of material strength. In other words, Michell [21] studied the minimum amount of material (in a lattice pattern) that structures need to contain to support a given system of forces applied to their components. Since Kumar [22] used a simplified methodology of optimized trusses to obtain the load path in deep RC beams, structural optimization has been extensively investigated (Kwak and Noh [23], Bołbotowsk and Sokó [24], Liang and Steven [25], Liang and Ng [26], and Guest and Moen [27]). The application of topological optimization concepts using finite element for plane stress problems started with Bendsoe and Kikuchi [28]. In that work, the problem of generating optimal topologies in structural design was addressed using a homogenization method. From this period, hundreds of publications appeared, resulting in several numerical TO methods that reached the stage of practical applications (Ramani [29], Blasques [30], Cui et al. [31], and Florea et al. [32]).

Automatic generation of optimal STMs in prestressed concrete beams by the Performance-Based Optimization (PBO) method was presented by Liang et al. [33]. The development of STM in prestressed concrete members is transformed into the TO problem of continuum structures. By treating prestressing forces as external loads, prestressed concrete beams can be analyzed, optimized, and sized by STMs. The study demonstrated that prestressing forces significantly modify the load transfer mechanism in structural concrete members. Moreover, partial prestressing offers a more economic design than conventional reinforcement or full prestressing.

The PBO of STMs in exterior and interior beam-column connections made of RC are presented by Liang [34]. Developing STMs in RC beam-column connections was treated as a TO problem. The optimal STM in a concrete beam-column connection was generated by gradually removing inefficient finite elements from the connection during an optimization process. It was demonstrated that the PBO is an effective tool for the design and detailing of structural concrete, particularly the D-regions.

Three methods using the genetic ESO algorithm were presented by Qiu and Liu [35] to automatically develop optimal STMs for deep beams. In the Finite Element Analysis (FEA) of the first method, the concrete and steel rebars are modeled by a plane element and a bar element, respectively. In the second method, the concrete and steel are assigned to two different plane elements, whereas in the third method only one kind of plane element is used with no consideration of the differences between the two materials. The results indicated that the third methodology presented the best ability in finding better sub-optimal results with less computational effort.

Lee et al. [36] presented effective layouts of materials reinforcement optimally placed into building frames for both static and dynamic problems. The followed methodology involved dividing the building structure into several regions to develop the optimization process. In this study, the TO method evaluated an optimal layout of reinforcement or redistribution of material to a specified volume in a given design space that maximized stiffness for a given set of loads and boundary conditions. Numerical applications inferred that the TO method is an applicable concept design tool to create effective layout designs for structural frames in construction industries.

Zhong et al. [37] presented an evaluation system for judging STM designed D-regions that was verified by different researchers. In this study, a ground structure methodology is used to generate the STM of a beam. The evaluation process was performed mainly based on two analytical tools, the ANSYS software and CAST (computer-aided strut-and-tie) design tool. During the process, the ANSYS software is mainly used to execute numerical simulations, such as crack propagation and load-carrying capacity test, while the CAST design tool is usually employed to determine the layout of reinforcing steel bars. Results indicated that the evaluation system is a reliable and efficient tool that can be used to evaluate different STM of the same D-regions design domain, especially for those concrete structures with no available experiment data.

A methodology for obtaining truss models automatically from the TO results was proposed by Xia et al. [38-40]. In [38-40], critical evaluations were made on the adequacy of the results of a continuous TO as a starting point for the design of STM structures of flat and three-dimensional models with physical non-linearity. Several examples from the literature obtained by STM were compared with the proposed model. In most cases, the results showed good performance, measured from proposed indices that assess the degrees of feasibility and economy of the truss. Resulting, from the optimization process, economically viable structures, and identifying non-viable truss structures in some of the analyses.

The maximum stiffness criterion to discover the optimal layout of ties in STMs was presented by Zhou et al. [41]. The minimum strain energy criterion and the maximum stiffness criterion have been proposed to determine the detailed layout of ties in optimal topology. It was demonstrated that the STM generated by the TO method is just a preliminary configuration because the RC is assumed to be a uniform elastic continuum. Thus, the effect of the reinforcing bars on the load path cannot be considered in the optimization process. The detailed layout of ties and struts in an STM cannot be determined directly from the optimal topology, which is only a preliminary configuration. Results indicated that the criterion of maximum stiffness is equivalent to the minimum strain energy criterion in most cases.



An improved element removal criterion based on the strain energy sensitivity was proposed along with the Windowed Evolutionary Structural Optimization (WESO) method by Wang et al. [42]. It was designed by using the Finite Element (FE) program ANSYS as the tool to effectively and accurately solve the TO problems of 2-D and 3-D structures. The proposed average strain energy density and the control parameters of average strain energy density were intended to define the minimum stress element range of discrete elements in the shortest time. It skipped the overall sorting process in the ESO method and achieved the goal of improving the optimization calculation efficiency. Most of TO algorithms rely on post-processing tasks to obtain a smooth final contour as they are based on finite elements. For most situations, this can be alleviated by using refined element meshes. Results indicated that its high-efficiency calculation process enabled more practical applications with good accuracy, by selecting high-order finite elements or a refined finite element mesh.

Novotny et al. [43], based on the publication by Bruyneel and Duysinx [44], observed that the standard formulation based on minimizing compliance under volume constraint becomes inadequate when self-weight loading is dominant. The authors introduced a regularization term for the compliance-based minimization problem that allows imposing any feasible volume constraint, leading to satisfactory results, avoiding trivial solutions and convergence problems. The effectiveness of the proposed approach in solving a structural TO problem under self-loading was demonstrated by the application of several numerical experiments.

Based on the Literature Review, there is a lack of papers that deal with RC TO, and in the few revised here, most used the TO for truss-like structure definitions in the STM. This work comes to propose a new view of the problem; in other words, just a few works propose a numerical solution for the design of the reinforcement of concrete structures after having a portion of the material removed from the design domain. In this context, the novelty of this paper is to bring a proposal to optimize RC structures with a two loop TO approach based on compliance and material strength.

3. Theoretical Basis

This paper uses a Bidirectional Evolutionary Structural Optimization (BESO) framework as a basis for the implementation of the RC TO. The domain is discretized using a 4-node quadratic isoparametric finite element for plane stress problems. The BESO formulation is that presented in Huang and Xie [19].

The main modifications include a two-loop formulation, wherein in the first loop, the concrete is topologically optimized based on a user-defined volume fraction, but irrespective of the stress state (as usual in standard TO). Also, in this first loop, the objective function is the compliance and the corresponding sensitivity number drives the TO. The final topology from this first loop is the design domain for the second loop and represents the stiffest structure for that prescribed volume fraction. In the second loop, the sensitivity number is changed to a p -norm value such that the steel can be exchanged with the failed concrete that comes from the first loop. This exchange of material is performed based on failure surfaces (Ottosen and von Mises) such that the stress state at any finite element is not violated. The convergence of the process is established when the previous constraint is fulfilled and the compliance of the structure stabilizes to a certain tolerance as in the first loop.

In the proposed methodology, the TO can be stated, for the first loop, as:

$$\begin{aligned} & \text{minimize } C = \mathbf{u}^T \mathbf{K} \mathbf{u} \\ & \text{subject to: } \mathbf{K} \mathbf{u} = \mathbf{F}, \quad v_f \times V - \sum_{i=1}^n V_i x_i = 0 \quad x_i = x_{min} \text{ or } x_i = 1 \end{aligned} \quad (1)$$

where C is the compliance of the structure; \mathbf{K} is the global stiffness matrix; \mathbf{u} and \mathbf{F} are the displacements and load vectors, respectively; v_f is the prescribed volume fraction; n is the effective finite element number; and x_i are the design variables (material density) for each element. To avoid ill-conditioned of \mathbf{K} matrix of the solution of structural problem, x_{min} is set as a small value (assumed 1×10^{-3} in this paper) instead of zero. In this loop, $x_i = x_{min}$ means voids and $x_i = 1$ represents concrete.

For the second loop, the optimization problem is stated as:

$$\begin{aligned} & \text{minimize } C = \mathbf{u}^T \mathbf{K} \mathbf{u} \\ & \text{subject to: } \mathbf{K} \mathbf{u} = \mathbf{F}, \quad \max(\sigma_i^{eq}) \leq \sigma_{lim}, \quad x_i = x_{min} \text{ or } x_i = 1 \end{aligned} \quad (2)$$

where σ_i^{eq} is the equivalent stress state that depends on the material (if the material is concrete (in this loop $x_i = x_{min}$), σ_i^{eq} is the Ottosen equivalent stress; if the material is steel (in this loop $x_i = 1$), σ_i^{eq} represents the von Mises equivalent stress) and σ_{lim} is the respective strength limit for the material.

In the usual multi-material TO, the stiffest material is the first material to occupy the design domain, and the other materials (ranked in a descending way order of stiffness) exchange with the remaining materials within the corresponding prescribed volume fraction in the topology obtained from the stiffest material. In the RC TO proposed, this order is inverted due to the fact the costs for concrete are much less than those for steel. Furthermore, the concrete should protect the steel against weathering and it is a material that easily is molded in almost any shape.

For the first loop, the elemental sensitivity number α_i^e used to drive the optimization is defined as the compliance at the element level, as:

$$\alpha_i^e = \frac{1}{2} \frac{\mathbf{u}_i^T \mathbf{k}_i \mathbf{u}_i}{V_i} = \frac{x^{p-1}}{2} \mathbf{u}_i^T \mathbf{k}_i^0 \mathbf{u}_i \quad (3)$$

where i means the element number; \mathbf{u}_i is the element displacement vector; \mathbf{k}_i is the element stiffness matrix; \mathbf{k}_i^0 with unit density; p is a penalty factor; and V_i is the element volume. As usual, a density penalization is used in this loop in the compliance minimization ($E_i = E_c x_i^p$). More details can be found in Huang and Xie [19] and Amaral et al. [45].

Whereas for the second loop, the elemental sensitivity number is defined as the p -norm of the equivalent stress ($\sigma_{eq,i}$), since this is analogous to a compliance criterion (Li and Steven [46]):

$$\alpha_i^e = \frac{(\sigma_{eq,i})^q v_i}{\sum_{i=1}^N (\sigma_{eq,i})^q v_i} \quad (4)$$

where q is a user-defined factor to highlight the stress state at the element level relative to the whole structure. This sensitivity number is further filtered at the node level using a mesh-independent filter based on the distance between a certain element and their neighbors. The parameter for this filter is the usual number of elements that represent the filter length (r_{min}). In the RC topology problems, the filter length will be defined separately for each loop.



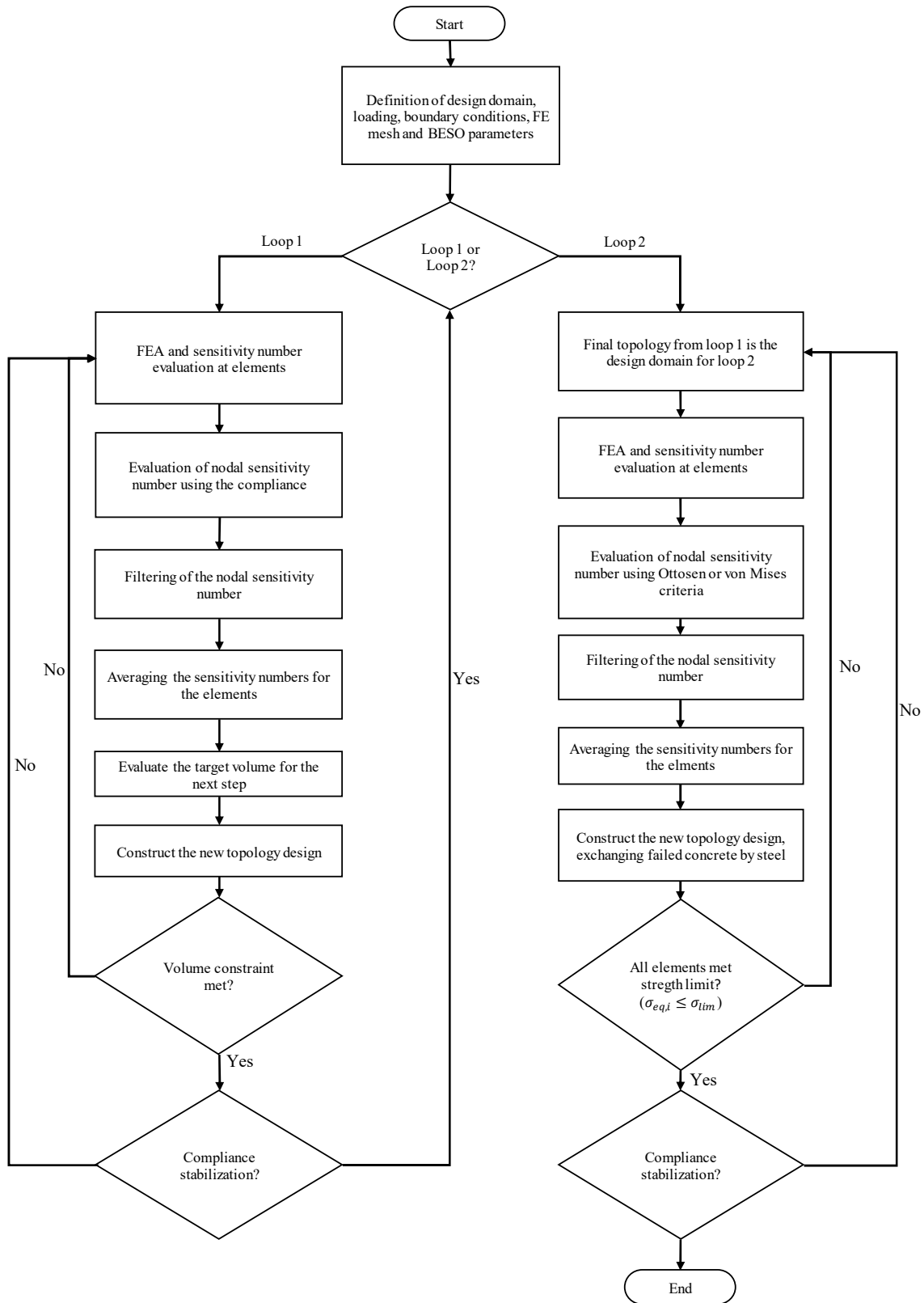


Fig. 1. Proposed two loops flowchart for RC TO.

The stress evaluations are made with the active elements, i.e., those elements that are not voids. If the element is concrete, the corresponding constitutive matrix is used, otherwise, if it is steel, the corresponding steel constitutive matrix is used instead. So, the high stress levels at void domain is not an issue in the analysis.

To account the material strength and assure that at the end of optimization any of the elements violates the strength limits σ_{lim} (for concrete, f_c ; for steel, f_y), the following failure criteria were used: for concrete the equivalent Ottosen stress (σ_{ott}) and for steel, the equivalent von Mises stress (σ_{vM}). The description of these surfaces are defined, respectively, as:

$$\sigma_{ott} = \alpha \frac{J_2}{f_{cm}} + \lambda \sqrt{J_2} + \beta I_1 \quad \text{and} \quad \sigma_{vM} = \sqrt{J_2} \tag{5}$$



where α , λ and β are parameters that are specified for a mean compressive strength of concrete (f_{cm}) (described in CEB-FIB [47]); J_2 is the second deviatoric tensor invariant; and I_1 is the first stress tensor invariant. Although this failure criteria is well-known and represents well the failure behavior, it does not account for scale length effects.

For the development of the optimization process based on the BESO method for RC structures, some hypotheses must be met: (i) the optimization of various materials in different loops; (ii) some strength criteria for each material; (iii) the objective function for the second loop, because the volume fraction is no longer a constraint of the problem but a natural result from the final stress constraints; and (iv) the sensitivity analysis approach, to determine the location of the material removed (Eq. 4) or exchanged (Eq. 5) from the computational domain.

Two optimization loops with different phases are proposed. Contrary to what was presented by Huang and Xie [19], in this study it was chosen the concrete material (less stiff and less expensive material) as the first phase of TO. The idea in this loop is only to reduce the structure weight, i.e., the designer will provide a constraint of volume to be reached by the algorithm while void elements are inserted in high compliance zones. Also, it is possible to have zones that will exceed the strength limit in concrete finite elements, which will be treated accordingly in the next loop. If the compliance is the objective to be minimized, the reasoning is to distribute the stiffer material first and then follow the less stiff, which means switching the two loops. As explained, in this paper this is not possible since the materials have to comply with stress constraints and structure's weight is another important factor. So, the volume fraction of concrete material is a parameter defined by the user and the final volume fraction for steel is a consequence of the fact the materials are complying with their strength. Besides that, concrete is the part that most contributes for the total inertia of the beam and the steel is the most expensive material to be employed.

In other words, the suggested process is divided into two loops, the first of which requires the user to provide the actual fraction volume they want to achieve. In this step, a stiffness sensitivity analysis is used to remove the material with higher compliance, which makes it possible for the concrete to experience stress levels above those allowed by the design. This problem will be solved in the second loop, where steel will replace the finite elements classified as concrete that reached a stress level that was too high by the standards set by the Ottosen criterion. Additionally, a von Mises criterion-based steel material verification is used. Only the topology produced in the first loop is used to build the optimization process in this loop. Also, the failed concrete material is replaced with steel material in the improved topology using a sensitivity analysis based on stress constraints. When there are no structural failures, the algorithm will stop the TO process; each finite element will then be examined for both failure criteria (steel and concrete). A summary of this explanation is presented in the flowchart in Fig. 1.

Concerning the ties of the structure, the regions where the steel material is being considered after the TO procedure, are members of STMs that are being subjected mainly to tensile forces carried by the steel. The steel rebars are calculated based on the resulting forces at the steel regions. In these regions, the principal stresses and their orientation (steel rebar direction) are evaluated. So, all the forces at the finite elements belonging a steel cross section are summed up to obtain a unique tension force in that steel cross-section. It is similar to the ties in the STM. Thus, the final steel area is obtained using this force and the yielding stress, divided by a safety factor (see Eq. (6)):

$$A_{s,min} = \frac{|\sum_{i=1}^N F_i|}{f_{yd}} \quad (6)$$

where $A_{s,min}$ is the resultant reinforcement area of steel for a given tie member; F_i is the resulting principal force in the i^{th} steel finite element in the critical cross section of the tie member; and f_{yd} is the design yielding stress for the steel material. During the process, the designer must locate highly stressed zones of the steel material to size the reinforcement for an arbitrary length of the structure. In addition, it was noticed that there are concrete regions subjected to compression-only in which the TO algorithm inserts steel due to the compressive failure of the material's strength ($\sigma_i^{Ot} > \sigma_{lim}^{concrete}$). The final steel rebars are obtained by rounding the values in Eq. (6) and choosing an adequate combination of commercial rebars.

For the improvement of the proposed methodology in the optimized RC topologies, a process of homogenization for the sized reinforcement regions (see Fig. 2), stipulated by the designer after the TO process, is considered in as a final step for the FEA. This was not necessary if the reinforcement was modeled as discrete bars linking nodes of the concrete finite element mesh or a model of embedded rebar. In the case of homogenized equivalent reinforced rebars, this allows to generate suitable reinforcement detailing for the final structure optimized and enables fair comparisons between final topologies. With the homogenization process, it will be possible to find the average properties from the composition of its constituents (concrete and steel materials), in the heterogeneous regions. In the end, in that regions, similar properties will be used for the computational domain that previously were considered only as steel material. This occurs because the discretized rebars will not occupy all the finite element volume and different configurations in rebar positioning will result in distinct steel to concrete area ratios. For this, it will be necessary to redefine the density for the finite elements in that regions from the resultant reinforcement design stipulated by the designer in relation to the total area of the finite element. Therefore, the homogenized densities in finite elements that are composed by some steel rebar and concrete, can be stated as:

$$\rho_h = \gamma\rho_s + (1 - \gamma)\rho_c \quad (7)$$

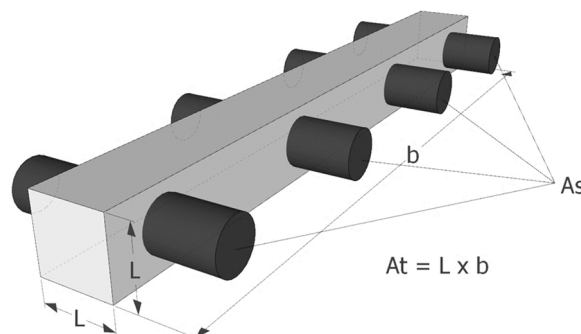


Fig. 2. Finite element with discrete reinforcement before the homogenization process (for plane stress state).



Table 1. Influence of $r_{min,1} = 3.5$ in topologies of RC when varying the volume fraction.

Iterations (1 st / 2 nd loop)	V_{target} [%]	RM_{conc} [%]	RM_{steel} [%]	C [Nm]	δ_{max} [m]	σ_{max}^{Ot} [MPa]	σ_{max}^{vM} [MPa]
28 / 43	50	35.50	14.50	9.63×10^2	-8.84×10^{-4}	25.78	150
22 / 48	60	47.10	12.90	8.72×10^2	-7.90×10^{-4}	30.07	140
8 / 33	70	54.50	15.50	7.82×10^2	-7.03×10^{-4}	26.88	138
6 / 39	80	64.80	15.20	7.20×10^2	-6.42×10^{-4}	31.00	114
4 / 46	90	72.90	17.10	6.74×10^2	-6.00×10^{-4}	25.39	133

Table 2. Influence of $r_{min,1} = 7$ in topologies of RC when varying the volume fraction.

Iterations (1 st / 2 nd loop)	V_{target} [%]	RM_{conc} [%]	RM_{steel} [%]	C [Nm]	δ_{max} [m]	σ_{max}^{Ot} [MPa]	σ_{max}^{vM} [MPa]
48 / 42	50	36.20	13.80	9.65×10^2	-8.87×10^{-4}	26.67	147
27 / 37	60	44.80	15.20	8.43×10^2	-7.63×10^{-4}	27.12	145
8 / 49	70	56.10	13.90	7.82×10^2	-7.03×10^{-4}	30.41	137
6 / 32	80	63.50	16.50	7.09×10^2	-6.32×10^{-4}	28.00	132
4 / 46	90	72.90	17.10	6.74×10^2	-6.00×10^{-4}	23.09	133

Table 3. Influence of $r_{min,1} = 10.5$ in topologies of RC when varying the volume fraction.

Iterations (1 st / 2 nd loop)	V_{target} [%]	RM_{conc} [%]	RM_{steel} [%]	C [Nm]	δ_{max} [m]	σ_{max}^{Ot} [MPa]	σ_{max}^{vM} [MPa]
25 / 44	50	35.10	14.90	10.57×10^2	-9.75×10^{-4}	27.17	164
23 / 41	60	46.70	13.30	8.64×10^2	-7.83×10^{-4}	29.10	155
8 / 36	70	53.90	16.10	7.73×10^2	-6.94×10^{-4}	26.15	142
6 / 32	80	64.20	15.80	7.21×10^2	-6.42×10^{-4}	28.57	131
4 / 39	90	72.90	17.10	6.82×10^2	-6.07×10^{-4}	22.76	111

Table 4. Influence of $r_{min,1} = 14$ in topologies of RC when varying the volume fraction.

Iterations (1 st / 2 nd loop)	V_{target} [%]	RM_{conc} [%]	RM_{steel} [%]	C [Nm]	δ_{max} [m]	σ_{max}^{Ot} [MPa]	σ_{max}^{vM} [MPa]
41 / 47	50	34.40	15.60	1.05×10^3	-9.63×10^{-4}	30.31	159
51 / 38	60	45.30	14.70	9.65×10^2	-8.82×10^{-4}	30.05	138
8 / 37	70	53.40	16.60	8.21×10^2	-7.38×10^{-4}	28.28	122
6 / 31	80	64.80	15.20	7.26×10^2	-6.49×10^{-4}	28.20	116
4 / 27	90	75.90	14.10	7.01×10^2	-6.25×10^{-4}	26.86	113

where ρ_h is the homogenized density; γ is the ratio of steel to concrete areas within a quadratic isoparametric finite element given by $\gamma = A_s/A_t$, being A_s is the resultant area of steel for the reinforcement design (for an length defined by the designer and accounting for an appropriate anchorage length) and A_t the total area of the element (given by $A_t = L \times b$); ρ_s is the steel density; and ρ_c is the concrete density.

Assuming a perfect bonding between concrete and steel, the homogenized Young's modulus E_h , is given by:

$$E_h = \gamma E_s + (1 - \gamma) E_c \quad (8)$$

This allows fair comparisons between the final topologies and rebar arrangements due to the equivalence in the total amount of steel area used in both designs.

4. Numerical Examples

4.1 Sensitivity Analysis of RC Topology Optimization Parameters

The geometry of the first analyzed structure is presented in Fig. 3(a) and is a RC deep beam. It is supported by columns of 600×450 mm and it is loaded by a concentrated load $F = 2415.6$ kN applied on a rigid bearing plate with dimensions of 450×450 mm. In the FEA, the self-weight of the structure is considered with densities of $\rho_s = 7780$ kg/m³ for the steel and $\rho_c = 2200$ kg/m³ for the concrete.

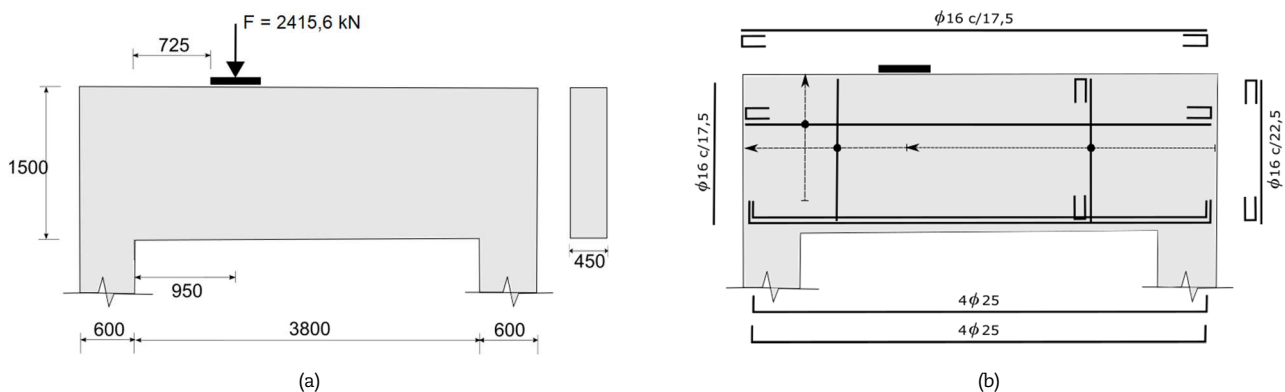


Fig. 3. (a) Deep beam geometry. (b) Reinforcement detailing according to Eurocode 2 for a STM (Adapted from Goodchild et al. [12]) (Dimensions in mm).



Regarding the material parameters, it is considered $f_y = 500$ MPa, $E_s = 210$ GPa, $\nu_s = 0.30$ for steel Rebars; C35 concrete, $E_c = 33$ GPa and $\nu_c = 0.20$ for the concrete; $E_v = \nu_v = 0$ for the voids. The Young's modulus and the yield strength limit are assumed constant within the finite element (evaluated at the element's center). Also, the concrete presents a uniaxial tensile strength of 3 MPa (parameters used for the Ottosen Four-Parameter criterion). The beam was designed using the usual Strut-and-Tie methodology according to Eurocode 2, as exposed by Goodchild et al. [12], and the result details of the proposed STM are presented in Fig. 3(b).

Four-node isoparametric finite elements with $L = 0.025$ m are used to discretize the computational domain of the structure, resulting in 12000 finite elements in the discretization of the domain ($N_x = 200$ and $N_y = 60$), so that the final structural model is sufficient for displacement and stress evaluation. The parameters adopted for the BESO method to investigate the influence of the filter scheme in a TO procedure were: (i) the penalization p for the compliance optimization ($p = 3$ as baseline for the 1st loop); (ii) the penalization of the degree of proportional stress q ($q = 4$ as baseline for the 2nd loop); (iii) the evolutive ratio ER_1 and ER_2 (assumed as baseline $ER_1 = 0.05$ for the 1st loop, $ER_2 = 0.01$ for the 2nd loop); (iv) the filter length scale; and (v) the final volumetric fraction. The parameter (iii) implies that the algorithm will remove 5% of the concrete volume of the structure in each iteration in the 1st loop, until the final volume fraction is reached. Also, 1% of failed concrete material will be exchanged by steel material at each iteration until the structure does not present any structural failure. Moreover, it was considered in all simulations an average sensitivity factor between iterations of $\mu = 0.5$ in order to stabilize the TO process. For the parameter (iv) it is adopted different length scales to determine the influence of the filter scheme in the final topologies, such as $r_{min,1} = 3.5, 7, 10.5,$ and 14 elements in the 1st loop, and $r_{min,2} = 3.5$ finite elements in the 2nd loop. It was tested final volume fractions of $V_{target} = 0.5, 0.6, 0.7, 0.8,$ and 0.9 to check the better V_{target} that minimizes the compliance C of the structure and shows a better manufacturability in terms of internal voids and identifiable members. The results of this first analysis are brought in Tables 1, 2, 3, and 4 allowing to investigate the influence of the length scale on final topologies. Each line represents one of the previously cited volume fractions. Also, RM_{conc} and RM_{steel} denote the remaining material of concrete and steel w.r.t. the initial design domain, respectively. The sum of these variables means the predefined target volume fraction V_{target} .

As can be seen in Tables 1, 2, 3 and 4, for an investigative analysis of the BESO parameters in the used methodology, it was observed that the filter scheme demonstrates a better minimization of the compliance value when small values $r_{min,1}$ are adopted in the 1st loop for this parameter. Regarding the variation of this parameter in the 2nd loop $r_{min,2}$, the optimization algorithm does not demonstrate a significant change in steel areas in the final optimized topology. However, there is a small increase in the remaining material of steel when the parameter $r_{min,2}$ is increased in the 2nd loop. In addition, it was noticed in the 1st loop that as $r_{min,1}$ parameter increases, large voids inside the optimized topology are formed and consequently it is less prone to form internal slender members that might harm fabrication. Thus, from a manufacturable perspective, it was noted that high values of this parameter $r_{min,1}$ must be adopted to better analyze the mechanical behavior of topologically optimized RC structures. In other words, the user has to choose the better tradeoff between manufacturability and higher stiffness topologies.

Regarding the analysis of the influence of the penalty factor (p) adopted for the 1st loop (optimization process based on compliance minimization), it was observed that this parameter has no influence on the final topology of RC structures. The reason is due to the compliance-based convergence criterion used to stabilize the optimization algorithm and the intrinsic behavior of the BESO method with no intermediate densities. With this, the algorithm converges always to a global optimal result irrespective of the p value. Concerning the penalty of the degree of stress proportion, adopted in the 2nd loop, this parameter demonstrates better stability with low values ($q = 1$ than $q \gg 1$), that is, no checkerboard pattern in the steel material was observed on the topology (see Fig. 4). It is well-known that the use of high q -value is desirable to avoid regions violating the strength of the material. However, by adopting a low value for the degree of a stress proportion (q), some of the finite elements classified as concrete may exceed the failure surface limit of Ottosen. Besides that, during the simulations, the results indicated that by using a low filter value ($r_{min,2}$) together with a high degree of a stress proportion value (q), it was possible to have better control of the maximum stress value in the concrete material in the optimized topology. In summary, the use of a low q -value result in a less prone checkerboard pattern, but with no guarantee in meeting the stress limit.

In sequence, the mechanical behavior of the topologies with a final volume fraction V_{target} of 0.9, 0.8, 0.7, 0.6, and 0.5 is discussed. For that, a reference optimized topology of the deep beam with no voids ($V_{target} = 1$) was used, see Fig. 5(a). In Fig. 6, the deflected form in vertical direction and the equivalent stress distribution of von Mises and Ottosen in the optimized topology with no voids are also presented.

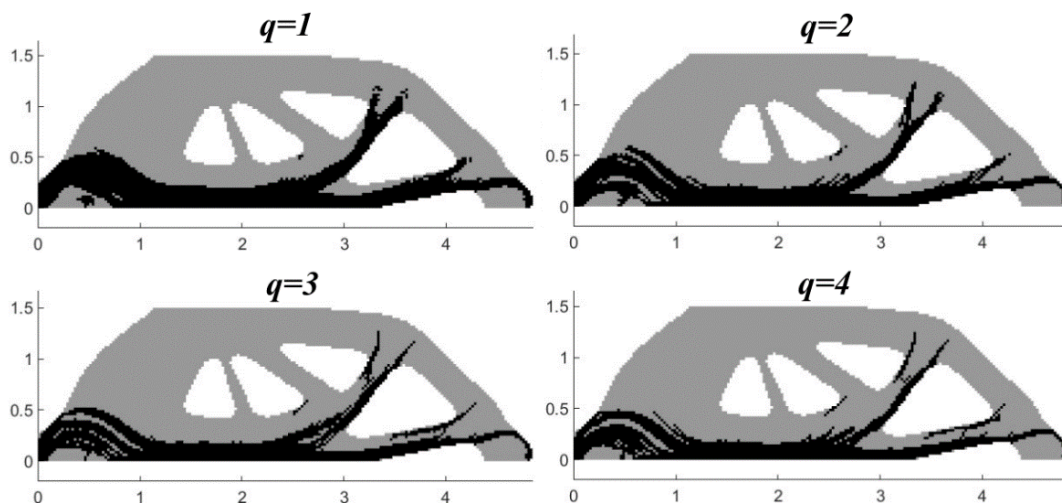


Fig. 4. Influence of q in topologies of RC for $V_{target} = 0.6$, $r_{min,2} = 3.5$.



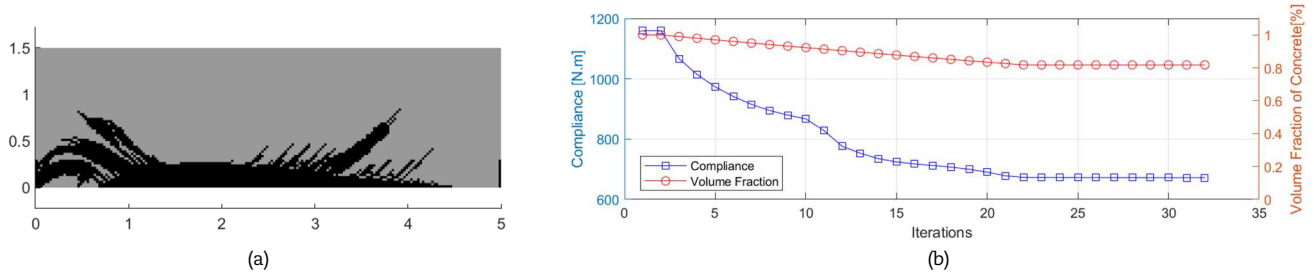


Fig. 5. (a) Final topology of the deep beam with no voids ($V_{target} = 1$ and no concrete TO); (b) Compliance and volume fraction of concrete along with iterations.

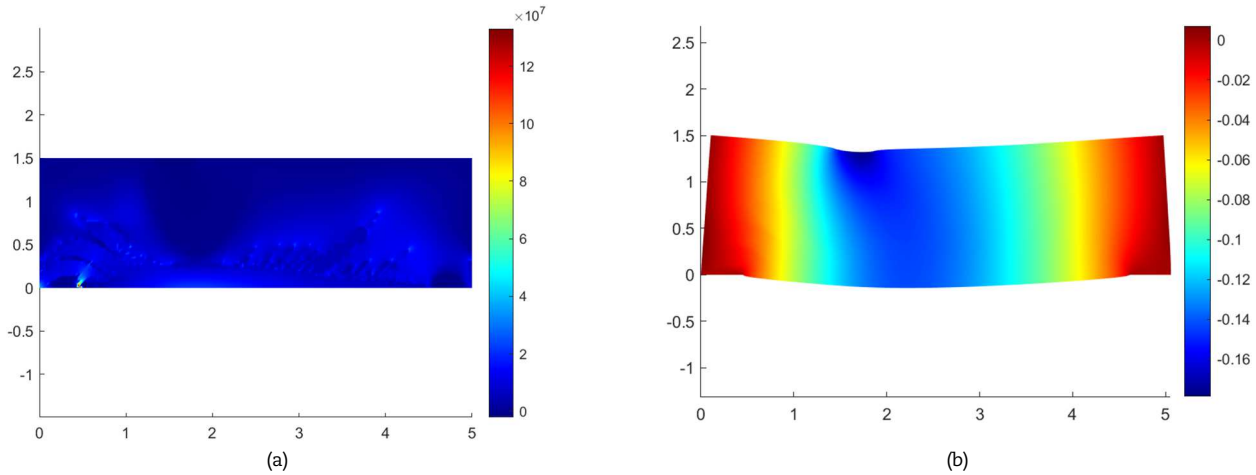


Fig. 6. (a) Equivalent stress distribution of von Mises and Ottosen (in Pa) and (b) deflected structure in y direction multiplied by a magnification factor (300), in m, of the final topology with no voids in the design domain.

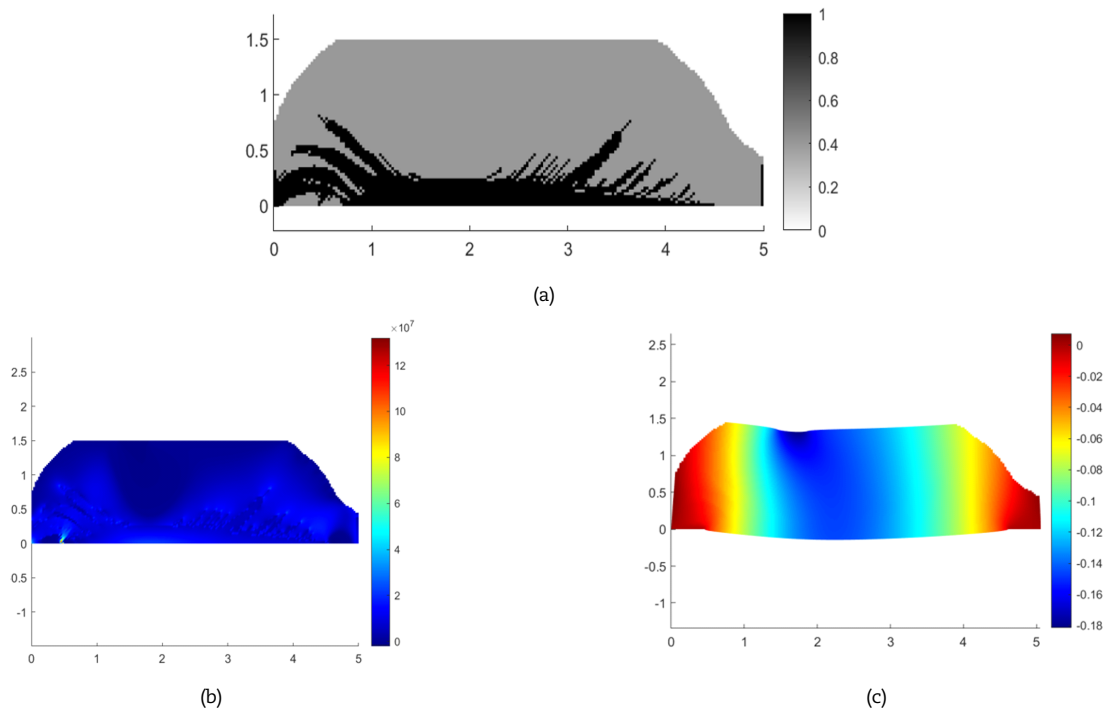


Fig. 7. (a) Final topology with $V_{target} = 0.90$ and its (b) equivalent von Mises and Ottosen stress distribution (in Pa) and (c) deflected structure in y direction multiplied by a magnification factor (300), in m.

A simulation reference topology with no voids was performed (which means no concrete during the TO process, but only steel optimization). The code in MATLAB resulted in $\sigma_{max}^{Ot} = 28.58 \times 10^6$ Pa (for the concrete material) and $\sigma_{max}^M = 115 \times 10^6$ Pa (for the steel material), which implies that all the domain is in a safe condition. Furthermore, concerning the maximum deflection δ_{max} of the topology, the topologically optimized structure meets the stiffness requirement of Eurocode 2, as it presents $\delta_{max} = 6.06 \times 10^{-4}$ m (being $\delta_{lim} = \text{span}/500$). Figure 5 (b) presents compliance and the volume fraction behavior of concrete along with iterations. The volume fraction in concrete in the 1st loop is $V_{target} = 1$ and the decrease in volume fraction occurs only in the 2nd loop and is due to the exchange of failed concrete material for steel in the optimized topology.



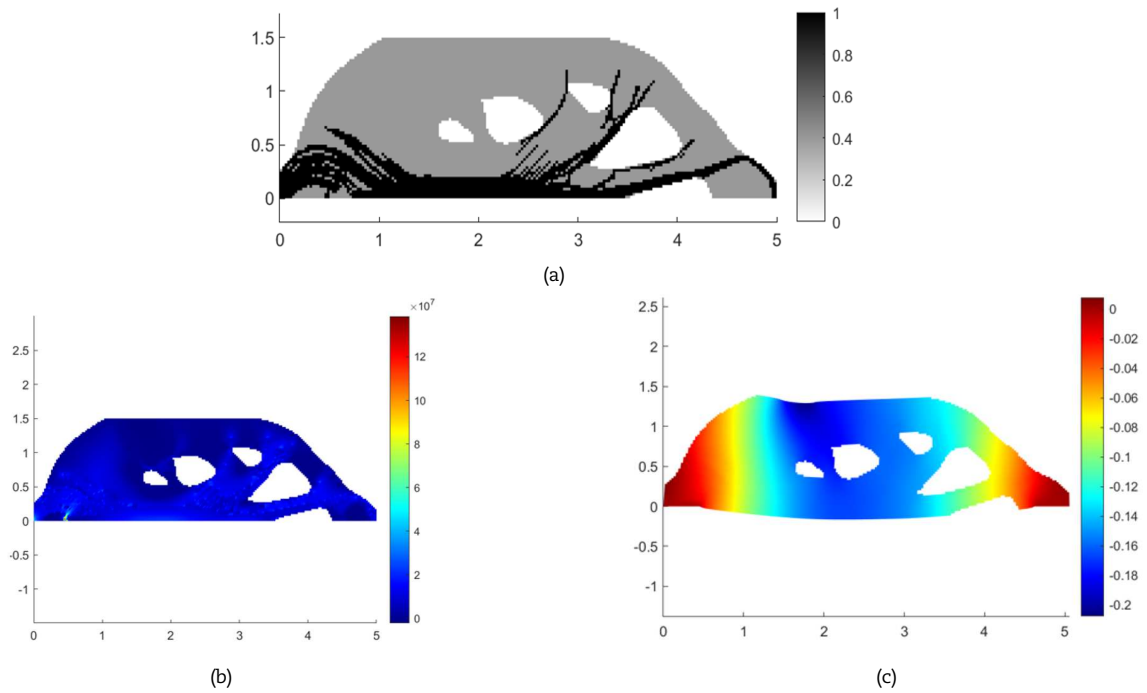


Fig. 8. (a) Final topology with $V_{target} = 0.70$ and its (b) equivalent stress distribution of von Mises and Ottosen (in Pa) and (c) deflected form in y direction multiplied by a magnification factor (300), in m.

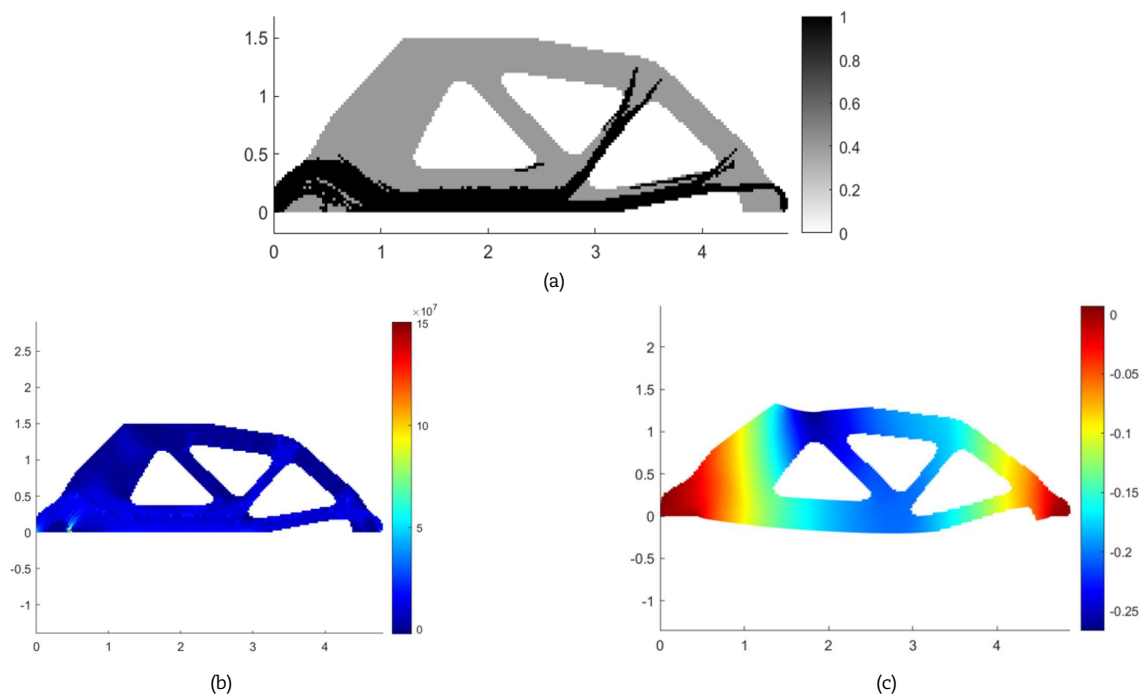


Fig. 9. (a) Final topology with $V_{target} = 0.50$ and its (b) equivalent von Mises and Ottosen stress distribution (in Pa) and (c) deflected structure in y direction multiplied by a magnification factor (300), in m.

Concerning the topologies with voids within the structure, Figs. 7, 8, and 9 present the mechanical response for the topologies with a final volume fraction of 0.9, 0.7, and 0.5, where gray represents concrete material, black represents steel material and white represents the voids within the computational domain. Moreover, for these simulations that consider voids within the computational domain, a value of $q = 5$, $r_{min,1} = 7.0$, and $r_{min,2} = 1.5$ were adopted because the concrete maximum stress remains around 75% of the failure surface limit of Ottosen for the proposed problem of the deep beam, which is desirable for safety purposes.

When comparing the topologies with voids ($V_{target} = 0.9$ to 0.5, see Figs. 7(a) to 9(a)) and the reference topology ($V_{target} = 1.0$, see Fig. 5(a)), it can be seen that all optimized structures present a similar behavior in the distribution of the equivalent of von Mises and Ottosen stresses (see Fig. 6(a) and 7(b) to 9(b)). Also, none of the topologies presented stress higher than the predefined stress limit (see also Tables 1 to 4). Regarding the principal stress regions, it was noticed that between the place of load application together with the places where the supports are considered, compression zones were created between these points (struts) in the topologically optimized structure (place with the highest percentage of concrete); and in the region between the supports, it was identified a tensile zone (ties, with the highest percentage of steel). For each finite element at plane stress, the principal stress and plane are evaluated and a graph with these principal stresses at the center of the finite element was plotted accordingly. Figure 10 summarizes the explanation of the principal stresses on the topologies with voids, where blue arrows are mainly in the compression zone and red arrows are mainly in the tensile zone.



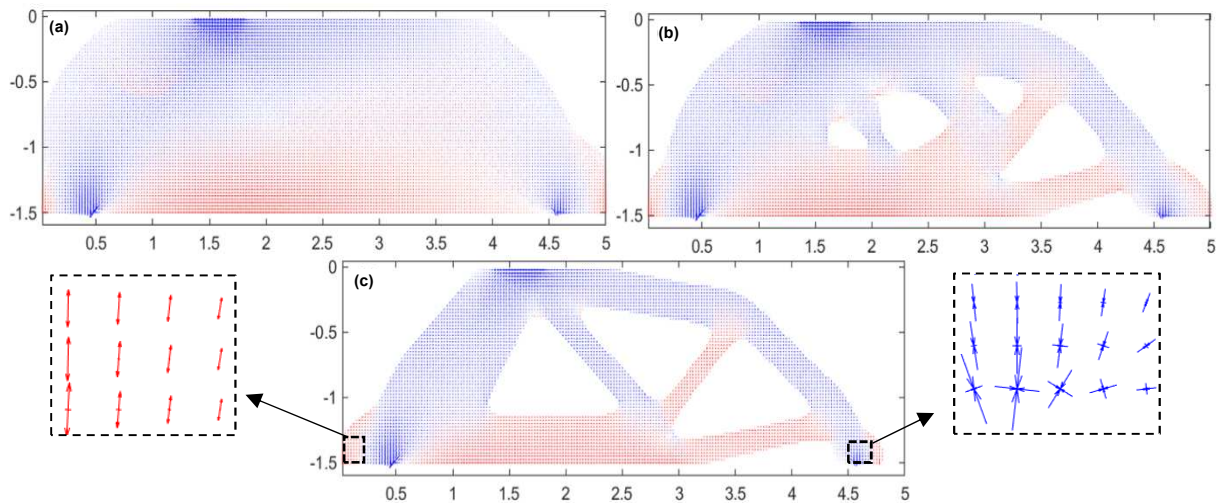


Fig. 10. Principal stress directions in optimized topologies with a final volume fraction of (a) 90%, (b) 70%, and (c) 50%. Blue arrows mean compression and red arrows mean tension.

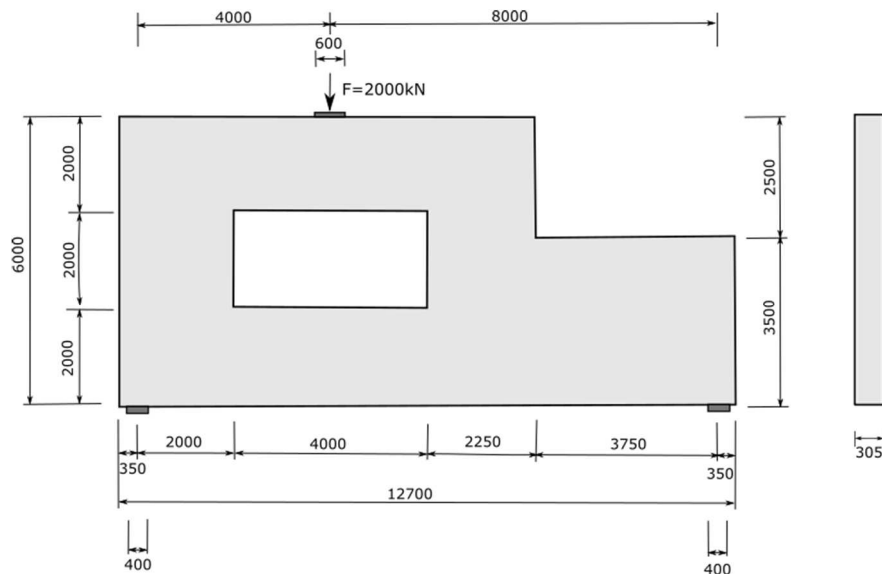


Fig. 11. Geometry of a deep beam with a hole (Adapted from Novak and Sprenger [48]).

Regarding the stiffness analysis of the topologically optimized deep beam (see Figs. 6(b) and 7(c) to 9(c)), the maximum deflection occurred at the place where the load was applied. Nevertheless, the vertical displacements at the midspan were even lower than this value, as can be seen in Fig. 6(b). Besides that, according to the Eurocode 2 standard, the maximum deflection located in the lower and central part of the beam should be below 0.01 m for the case of quasi-permanent loads (dead + characteristic live loads). Thus, referring to Table 1 to 4, when analyzing all the results obtained for the volumetric fractions of 0.5, 0.6, 0.7, 0.8, and 0.9 of material retained in the computational domain, it can be seen that the deflection requirements of the standard are met for all the analyzed optimized topologies cases.

4.2 Topology Optimization of a Deep Beam with a Hole designed according to ACI318:2002

The methodology presented in this paper was implemented in one example of a deep beam with a hole (see Fig. 11, dimensions in mm) found in Novak and Sprenger [48]. The idea was to develop a comparison between the final topology of the proposed methodology with the structure designed with STM and ACI318:2002, aiming to obtain lighter structural elements without reaching the surface failure criteria for any material.

From Fig. 11, the deep beam with a hole has dimensions of 12700 × 6000 × 305 mm with an opening of 4000 × 2000 mm and an asymmetry in the upper right corner of 4100 × 2500 mm. The beam is supported on pillars with dimensions of 400 × 305 mm. At the place where the load $F = 2000$ kN was applied, there is a plate with the following dimensions 600 × 305 mm. In addition, it was adopted the following parameters for the concrete: the design strength to compression f_{cd} and tensile f_{ct} are 31 MPa and 3 MPa, respectively; elastic modulus E_c is 31 GPa, the Poisson ratio's ν_c is 0.22; and a density ρ_c of 2400 kg/m³; while, for the steel: yield stress f_{yd} is 368 MPa, the Poisson ratio's ν_c is 0.30, and a density ρ_c of 7780 kg/m³. The steel covering is assumed as a length of one finite element. The resulting sizing of the STM obtained by Novak and Sprenger [48] is showed in Fig. 12.

Table 5 presents the optimization parameters used for the BESO approach. Also, 2D four-node quadrilateral finite elements with a size of $dx^e = dy^e = 0.050$ m are used to discretize the computational domain, such that the structural model presents a good accuracy in displacement and stress. Thus, 30480 finite elements are used for its discretization ($N_x = 254$ elements and $N_y = 120$ elements).



Table 5. Parameters for the BESO method.

Loop	r_{min}	V_{target}	ER	x_{lim}	p	q	α	tol	Maximum iteration
1 st	4	0.8	0.02	[0,1]	3	4	0.5	10^{-6}	100
2 nd	3	0.0	0.01						

The first analysis is exposed in Fig. 13. In Fig. 13(a), it was observed that the compliance stabilizes when the target volumetric fraction of 0.8 was reached. It is worth remembering that at this stage there are only concrete elements and voids. In the 2nd loop, compliance reduces until reaching the minimum strain energy and stabilizes when the structure is the stiffest for the desired volumetric fraction. The volumetric fraction reduces a little more than 0.8 due to the replacement of failed concrete elements with steel elements in the 2nd loop.

In Fig. 13 (b), failed material is represented by residue > 0 (residue = $\sigma_{eq}/\sigma_{lim} - 1$) and safe material with stress levels below the limit stress represented by residue ≤ 0. In the 1st loop, the concrete exceeds its strength, as observed in the residue close to 2, and has high stresses, above 95 MPa. When the 2nd loop starts and the steel starts to be allocated in the structure, both the maximum stress and the residue related to the Ottosen stress are below their limit values, indicating that the concrete material is not under failure. The same applies to steel, where both the maximum stress and the residual related to von Mises stress are below its yield value.

Next, Fig. 14(a) shows the optimized topology of the deep beam, with $V_{target} = 0.8$, containing regions with openings (white), concrete (grey) and steel (black); and, Fig. 14(b) the equivalent Ottosen and von Mises stresses distributed along the optimized structure. As seen in Fig. 14(b), after the optimization process is over, the maximum stress in the structure (steel) is around 26 MPa, which are some red dots shown in Fig. 14(b). Together with the graph in Fig. 14(a), it was possible to notice that they are regions with steel elements under tension and that there was an overall relief in the maximum stresses due to the optimization process. The maximum stress in concrete was around 24 MPa.

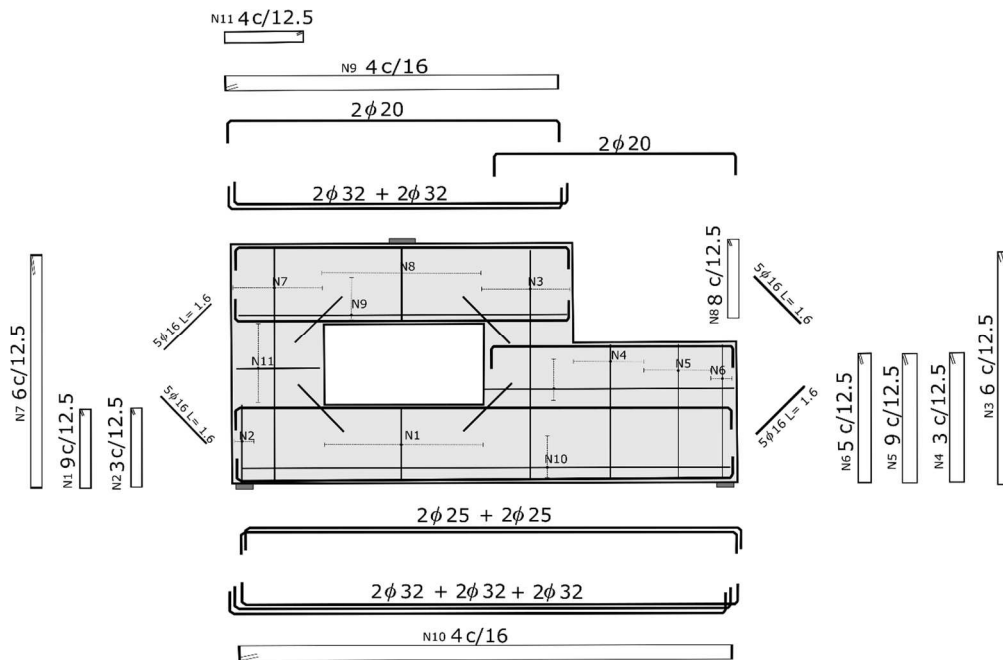


Fig. 12. Deep beam sized with STM following ACI 318:2002 (Adapted from Novak and Sprenger [48]).

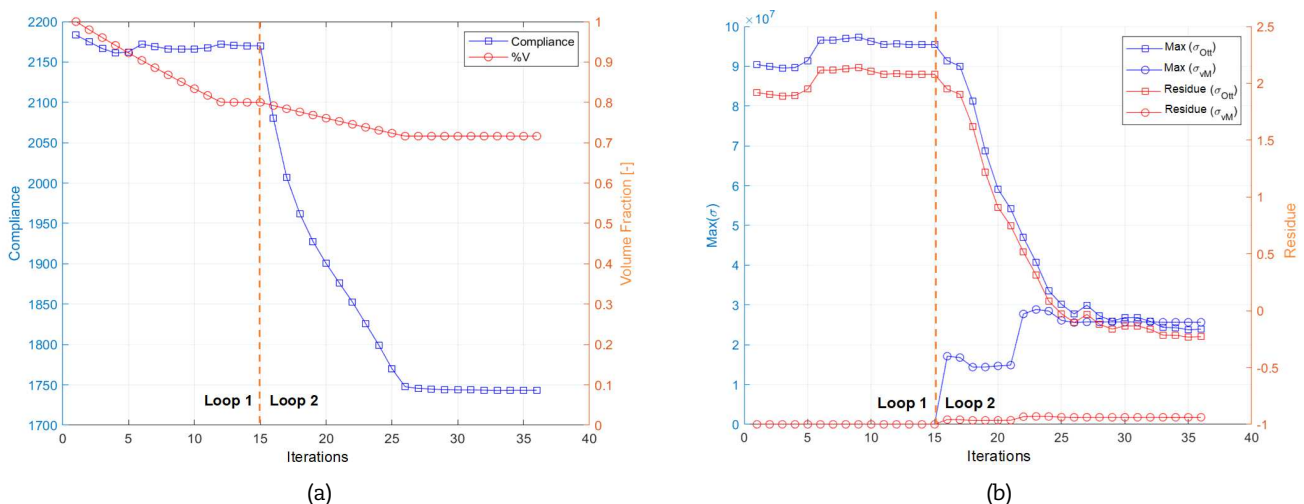


Fig. 13. (a) Compliance (N.m) and volumetric fraction curve versus iterations and (b) Maximum stress (in Pa) and residual curve versus iterations.



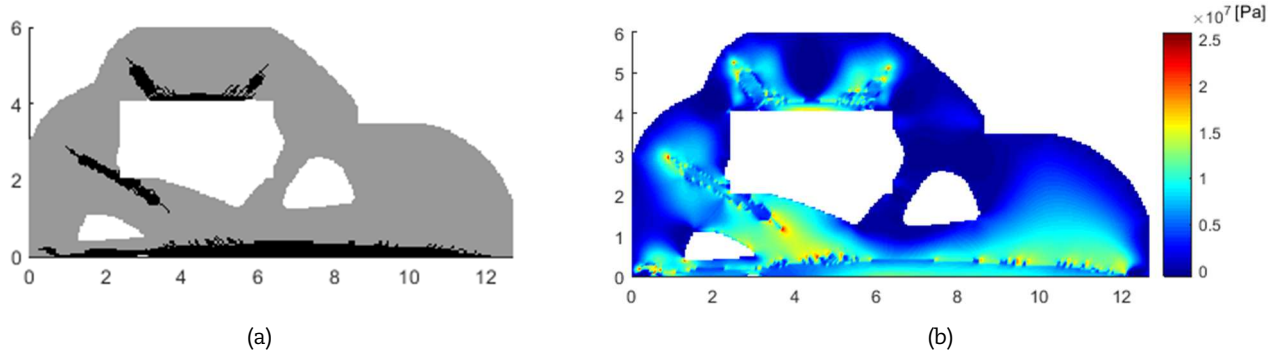


Fig. 14. (a) Optimized topology of a deep beam with a hole and (b) Ottosen and von Mises smoothed equivalent stresses.

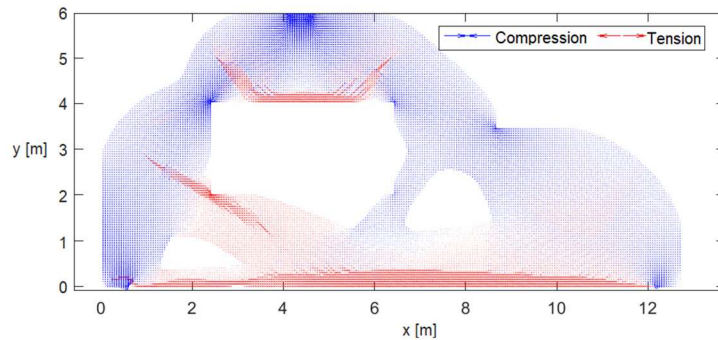


Fig. 15. Principal stress directions in the optimized topology in the case of deep beam with a hole.

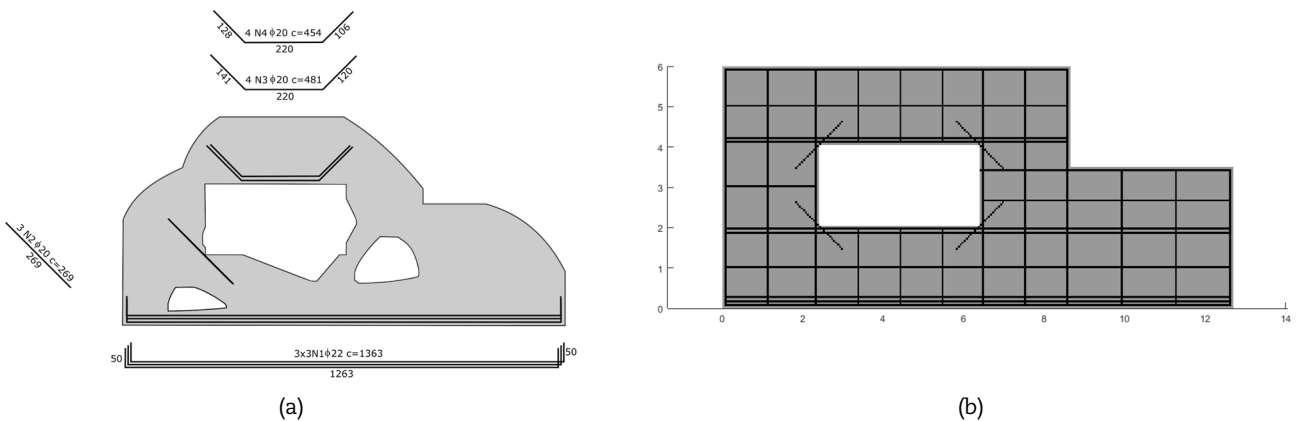


Fig. 16. (a) Final detailing of this work using TO and (b) a simplification of detailing proposed by Novak and Sprenger [48].

Figure 15 indicates the directions of the principal tensile and compressive stresses that occur in the structure. The regions in light red are regions with slightly tensioned concrete, not failed; the regions with the dark red are regions where there was an exchange of concrete with steel and finally the regions in blue are regions mainly under compression. It is clear that in supports and point load are the most compressed regions of the structure.

After verifying the optimized structure in terms of stress levels, the sizing and detailing stage begins, since the resulting optimized structure (Fig. 14(a)) does not match the requirements for manufacturing, e.g., standard coverings should be met and equivalent commercial bars should be used. Table 6 presents the steel area for the optimized structure.

Table 6. Sizing of the reinforcement for the optimized deep beam.

Rebar	F_u [kN]	$A_{s,nesc}$ [mm ²]	ϕ [mm]	N ^o of rebars	$A_{s,form}$ [mm ²]	Spacing [cm]	Length [m]	Distribution
N1	344	1109	22	3	1140.3	8.45	1.63	3 ϕ 22
N2	344	1109	22	3	1140.3	8.45	13.63	3 ϕ 22
N3	344	1109	22	3	1140.3	8.45	13.63	3 ϕ 22
N4	363	1169	20	4	1256.8	5.17	4.81	4 ϕ 20
N5	363	1169	20	4	1256.8	5.17	4.54	4 ϕ 20
N6	259	833.5	20	3	942.6	8.75	2.69	3 ϕ 20



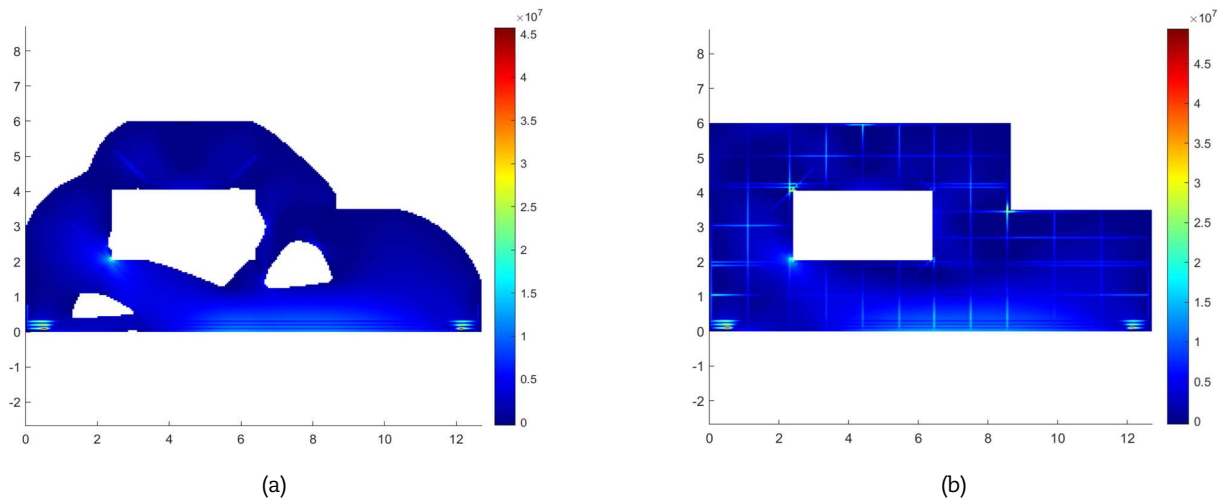


Fig. 17. Ottosen and von Mises smoothed equivalent stresses acting on the deep, in Pa, with (a) the proposed reinforcement and (b) sized by Novak and Sprenger [48].

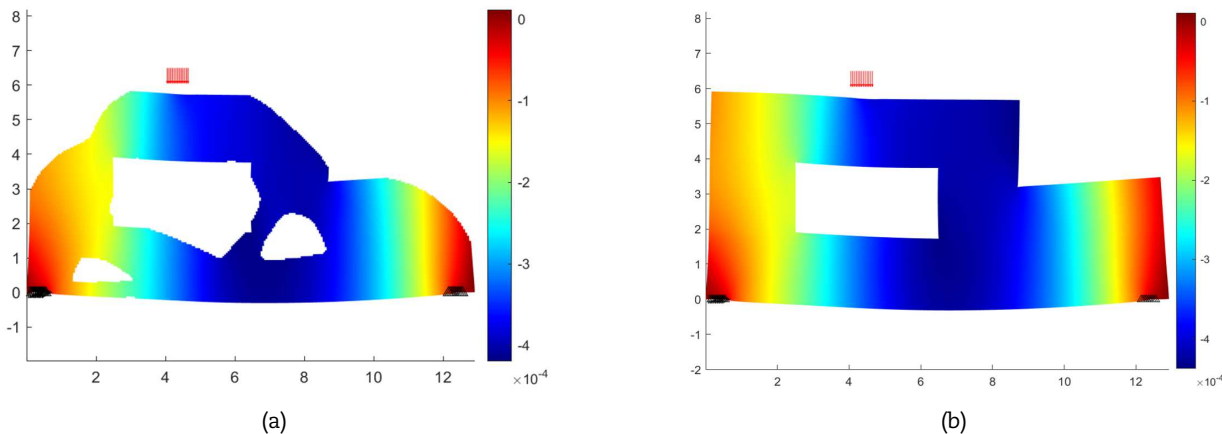


Fig. 18. Deflected configuration of the deep beam with (a) proposed reinforcement and (b) sized by Novak and Sprenger [48].

Thus, Fig. 16(b) shows the idealized discretization by Novak and Sprenger [48] previously showed in Fig. 12, and the rebar areas and numbers are the same in the previous Figure. Figure 16(a) illustrates the proposed detailing from the TO structure. A finite element analysis was performed to generate the values of stresses and displacements for comparison with Novak and Sprenger [48] detailing and the proposed for a TO structure in this work. In Fig. 16(b), the original bars were condensed into elements of the same length and area. A simplification of the reinforcement distribution was performed in the detailing in order to simplify groups of rebars in the same cross-section height. It is worth remembering that the comparisons were performed by the same analysis code, avoiding differences that would eventually occur if one uses different codes.

With the two structures detailed and discretized, it was possible to generate results concerning the stress distributions (Fig. 17) and the deformed configuration (Fig. 18). To keep the analysis in the elastic-linear regime, it was considered 10% of the acting load.

According to the results of Fig. 17, the stress in concrete is 27 MPa and in steel is 46 MPa. In the structure designed by Novak and Sprenger [48], a stress of 17 MPa on the concrete and 49 MPa on the steel acts. In both cases, these limit values are restricted to the support regions of the structure and corners of the central opening, and these same values are much smaller in the other regions of the structure.

Regarding the displacements, the proposed structure presented a maximum displacement $\delta = 0.41$ mm (see Fig. 18(a)), while the structure designed by Novak and Sprenger [48] presented a maximum displacement $\delta = 0.46$ mm. (see Fig. 18(b)) Comparatively, the displacements of the structures are small and close to each other, indicating that the structures will be stiff enough to resist the reduced loading.

Finally, after evaluating the mechanical behavior of the deep beam, a comparison was made concerning cost, volume and mass between the optimized beam (for $V_{target} = 0.80$) and that sized by the STM.

For the structure sized by STM, the volume of steel resulted in 1.26% of the total volume. In this case the total volume is $V_{STM} = 17.67$ m³, and the final mass (including steel and concrete) was $m_{STM} = 43618$ kg. For the proposed TO structure the volume and mass of the structure were determined. In this case the total volume is $V_{TO} = 14.14$ m³, and a final mass (including steel and concrete) was $m_{STM} = 34262$ kg. In terms of volume and mass, the structure with discrete bars proposed by this work has 20% less volume and 21.5% less mass.

For comparisons purposes, a fictitious monetary unit \$ was used which resembles the costs proportions for steel and concrete in a particular country. In terms of costs, it was assumed \$469/m³ for a C30 concrete and \$10/kg for CA-50 steel. The final costs are $C_{STM} = \$25511$ and $C_{TO} = \$11333$, for the STM designed structure and TO designed structure, respectively. Therefore the proposed TO structure allowed a reduction in final cost of around 56% if compared with the STM structure.



5. Conclusions

A new methodology to size the reinforcement of TO Reinforced Concrete structures was presented in this paper. To do so, a TO procedure for multi-materials was developed using the BESO method. At first, the methodology maximizes structural stiffness, for a desired volume fraction (reducing weight), and in the next step, it determines the internal steel/concrete distribution according to a p -norm stress criterion. Once the optimization process finishes, the reinforcement detailing process takes place, which uses the sum of the principal forces obtained from the finite element analysis in steel material regions (as occurs with the tie in the STM methodology).

For the analyzed examples, in the first case (a deep beam with no opening), it was demonstrated the influence of the BESO parameters on RC. In this study, it is clear that the designer must choose the best trade-off between manufacturability and high stiffness for topologies made of RC. Furthermore, when evaluating the mechanical behavior of the optimized topologies, some of the requirements of the Eurocode 2 (2004) standard were verified, such as displacements and stress limit states constraints. Also, it can be seen that in between the supports and applied loads, compression/tension zones are created in the TO structure that resembles the members assumed in the STM truss structure. The link between the formed members are zones that presents a biaxial compression/tension state.

In the second example, a deep beam with openings and discontinuities was analyzed concerning the final cost, mass and volume. This deep beam was previously designed using ACI318:2002 and the STM method. The same beam was topologically optimized using the proposed methodology in this paper. It was found that the optimized structure presents a reduction of 20% of the total volume and a reduction of 21.5% of mass. These reductions led to a cost saving of 56%. Furthermore, it was found that the optimized structure had a maximum vertical displacement 11% smaller than the non-optimized structure. It is believed that this is due to the non-optimized structure have more material in its geometry which results in more weight and, consequently, a higher vertical displacement. It should be emphasized that the self-weight is being considered during the analyses. It is noteworthy that the TO structure should have the same performance as the non-optimized structure, presenting similar stresses and displacements but with costs savings.

Future efforts are planned to include the analysis of other structural types (such as footings, corbels, and pile-caps), the implementation of embedded reinforcements for concrete finite elements, and an update of the code to handle nonlinear analysis.

Author Contributions

Rodrigo Reis Amaral initiated the project, developed the topology optimization design of experiments, and analyzed the results; Julian Alves Borges verified the code for the topology optimization and stress evaluation with finite elements; Walter Jesus Paucar Casas and Liércio André Isoldi verified the code for the finite element analysis and contributed to the revision of the final version of the paper; Herbert Martins Gomes planned and revised the Topology Optimization code in MATLAB, analyzed the results and led the project. The manuscript was written through the contribution of all authors. All authors discussed the results, reviewed, and approved the final version of the manuscript.

Acknowledgments

This study was financed in part by the CAPES (Coordination for the Improvement of Higher Education Personnel) – Finance Code 001. The authors also thank CNPq (Brazilian National Council for Scientific and Technological Development).

Conflict of Interest

The authors declared no potential conflicts of interest concerning this article's research, authorship, and publication.

Funding

The authors received no financial support for this article's research, authorship, and publication.

Data Availability Statements

The datasets generated and/or analyzed during the current study are available from the corresponding author on reasonable request.

References


- [1] Liang, Q.Q., Xie, Y.M., Steven, G.P., Topology Optimization of Strut-and-Tie Models in Reinforced Concrete Structures Using an Evolutionary Procedure, *ACI Structural Journal*, 97, 2000, 322-332.
- [2] Nagarajan, P., Pillai, T.M.M., Development of strut and tie models for simply supported deep beams using topology optimization, *Journal of Structural Engineering (Madras)*, 30, 2008, 641-747.
- [3] Xia, Y., Langellar, M., Hendriks, M.A.N., Automated optimization-based generation and quantitative evaluation of Strut-and-Tie models, *Computers & Structures*, 238, 2020, 106297.
- [4] Lanes, R.M., Greco, M., Guerra, M.B.B.F., Strut-and-tie models for linear and nonlinear behavior of concrete based on topological evolutionary structure optimization (ESO), *IBRACON Structures and Materials Journal*, 12, 2019, 87-100.
- [5] Xia, Y., Langellar, M., Hendriks, M.A.N., A critical evaluation of topology optimization results for strut-and-tie modeling of reinforced concrete, *Computer-Aided Civil and Infrastructure Engineering*, 35, 2020, 850-869.
- [6] Cedrim M.B.M., Lages, E.N., Barboza, A.S.R., Proposition and analysis of strut and tie models for short corbels from techniques of topology optimization, *IBRACON Structures and Materials Journal*, 14, 2021, 14212.
- [7] Lee, D.-K., Yang, C.-J., Starossek, U., Topology design of optimizing material arrangements of beam-to-column connection frames with maximal stiffness, *Scientia Iranica*, 19, 2012, 1025-1032.
- [8] Shobeiri, V., Ahmadi-Nedushan, B., Bi-directional evolutionary structural optimization for strut-and-tie modelling of three-dimensional structural concrete, *Engineering Optimization*, 49, 2017, 2055-2078.
- [9] Dey, S., Karthik, M.M., Modelling four-pile cap behaviour using three-dimensional compatibility strut-and-tie method, *Engineering Structures*, 198, 2019, 109499.
- [10] Almeida, V.S., Simonetti, H.L., Neto, L.O., The strut-and-tie models in reinforced concrete structures analysed by a numerical technique, *IBRACON Structures and Materials Journal*, 6, 2013, 139-157.
- [11] El-Metwally, S.E., Chen, W.-F., *Structural Concrete: Strut-and-Tie Models for Unified Design*, Taylor & Francis Group, 2018.
- [12] Goodchild, C.H., Morrison, J., Vollum, R.L., *Strut-and-tie Models – How to design concrete members using strut-and-tie models in accordance with Eurocode 2*,





MPA The Concrete Centre, 2014.


- [13] Reineck, K.-H., *ACI SP-208, Examples for the Design of Structural Concrete with Strut-and-tie Models*, American Concrete Institute, 2002.
- [14] Wight, J.K., *Reinforced Concrete – Mechanics and Design*, Pearson Education, Inc., 2015.
- [15] Bendsøe, M.P., Sigmund, O., *Topology Optimization: Theory, Method and Application*, Springer, Berlin, 2003.
- [16] Da, D., Xia, L., Li, G., Huang, X., Evolutionary topology optimization of continuum structures with smooth boundary representation, *Structural and Multidisciplinary Optimization*, 57, 2018, 2143-2159.
- [17] Fu, Y.-F., Rolfe, B., Chiu, L.N.S., Wang, Y., Huang, X., SEMDOT: Smooth-edged material distribution for optimizing topology algorithm, *Advances in Engineering Software*, 150, 2020, 102921.
- [18] Biyikli, E., To, A.C., Proportional Topology Optimization: A New Non-Sensitivity Method for Solving Stress Constrained and Minimum Compliance Problems and Its implementation in MATLAB, *PLoS ONE*, 10, 2015, 0145041.
- [19] Huang, X., Xie, Y.M., *Evolutionary topology optimization of continuum structures: methods and applications*, John Wiley & Sons, UK, 2010.
- [20] Sethian, J.A., Wiegmann, A., Structural boundary design via level set and immersed interface methods, *Journal of Computational Physics*, 2, 2000, 489-528.
- [21] Michell, A.G.M., The limits of economy of material in frame-structures, *The London, Edinburgh, and Dublin Philosophical Magazine and Journal of Science*, 8, 1904, 589-597.
- [22] Kumar, P., Optimal force transmission in reinforced concrete deep beams, *Computers and Structures*, 8, 1978, 223-229.
- [23] Kwak, H.G., Noh, S.H., Determination of strut-and-tie models using evolutionary structural optimization, *Engineering Structures*, 28, 2006, 1440-1449.
- [24] Bojbotowski, K., Sokół, T., New method of generating Strut and Tie models using truss topology optimization, *PCM-CMM-2015 – 3rd Polish Congress of Mechanics & 21st Computer Methods in Mechanics*, 2, 2015, 625-626.
- [25] Liang, Q.Q., Steven, G.P., A performance-based optimization method for topology design of continuum structures with mean compliance constraints, *Computer Methods in Applied Mechanics and Engineering*, 191, 2002, 1471-1489.
- [26] Liang, Q.Q., Ng, A.W.M., Performance-based optimization of strut-and-tie models in reinforced concrete deep beams, *Innovations in Structural Engineering and Construction, Proceedings of the Fourth International Structural Engineering and Construction Conference*, 2007.
- [27] Guest, J.K., Moen, C.D., Reinforced concrete design with topology optimization, *19th Analysis & Computation Specialty Conference*, 2010.
- [28] Bendsøe, M.P., Kikuchi, N., Generating optimal topologies in structural design using a homogenization method, *Computer Methods in Applied Mechanics and Engineering*, 1, 1988, 197-224.
- [29] Ramani, A., Multi-material topology optimization with strength constraints, *Structural and Multidisciplinary Optimization*, 43, 2011, 597-615.
- [30] Blasques, J.P., Multi-material topology optimization of laminated composite beams with eigenfrequency constraints, *Composite Structures*, 111, 2014, 45-55.
- [31] Cui, M., Chen, H., Zhou, J., Wang, F., Multi-material proportional topology optimization based on the modified interpolation scheme, *Engineering with Computers*, 34, 2017, 287-305.
- [32] Florea, V., Pamwar, M., Sangha, B., Kim, Y., 3D multi-material and multi-joint topology optimization with tooling accessibility constraints, *Structural and Multidisciplinary Optimization*, 60, 2019, 2531-2558.
- [33] Liang, Q.Q., Xie, Y.M., Steven, G.P., Generating optimal strut-and-tie models in prestressed concrete beams by performance-based optimization, *ACI Structural Journal*, 98, 2001, 226-232.
- [34] Liang, Q.Q., Performance-based optimization of strut-and-tie models in reinforced concrete beam-column connections, *Real Structures: Bridges and Tall Buildings, Proceedings of the Tenth East Asia-Pacific Conference on Structural Engineering and Construction*, 2006.
- [35] Qiu, Y., Liu, X., Comparison on construction of strut-and-tie models for reinforced concrete deep beams, *Journal of Central South University of Technology*, 18, 2011, 1685-1692.
- [36] Lee, D.K., Yang, C.J., Starossek, U. Topology design of optimizing material arrangements of beam-to-column connection frames with maximal stiffness, *Scientia Iranica*, 19, 2012, 1025-1032.
- [37] Zhong, J.T., Wang, L., Deng, P., Zhou, M., A new evaluation procedure for the strut-and-tie models of the disturbed regions of reinforced concrete structures, *Engineering Structures*, 148, 2017, 660-672.
- [38] Xia, Y., Langelaar, M., Hendriks, M.A.N., Automated optimization based generation and quantitative evaluation of strut-and-tie models, *Computers and Structures*, 238, 2020, 106297.
- [39] Xia, Y., Langelaar, M., Hendriks, M.A.N., A critical evaluation of topology optimization results for strut-and-tie modeling of reinforced concrete, *Computer-aided Civil and Infrastructure Engineering*, 35, 2020, 850-869.
- [40] Xia, Y., Langelaar, M., Hendriks, M.A.N., Optimization-based three-dimensional strut-and-tie model generation for reinforced concrete, *Computer-aided Civil and Infrastructure Engineering*, 36, 2020, 526-543.
- [41] Zhou, L., He, Z., Liu, Z., Investigation of optimal layout of ties in STM developed by topology optimization, *Structural Concrete*, 17, 2016, 175-182.
- [42] Wang, L., Zhag, H., Zhu, M., Chen, Y.F., A new Evolutionary Structural Optimization method and application for aided design to reinforced concrete components, *Structural and Multidisciplinary Optimization*, 62, 2020, 2599-2613.
- [43] Novatny, A.A., Lopes, C.G., Santos, R.B., Topological derivative-based topology optimization of structures subject to self-weight loading, *Structural and Multidisciplinary Optimization*, 63, 2021, 1853-1861.
- [44] Bruyneel, M., Duysinx, P., Note on topology optimization of continuum structures including self-weight, *Structural and Multidisciplinary Optimization*, 29, 2005, 245-256.
- [45] Amaral, R.R., Borges, J.A., Gomes, H.M., Proportional topology optimization under reliability-based constraints, *Journal of Applied and Computational Mechanics*, 8, 2022, 319-330.
- [46] Li, Q., Steven, G.P., Xie, Y.M., On equivalence between stress criterion and stiffness criterion in evolutionary structural optimization, *Structural Optimization*, 18, 1999, 67-73.
- [47] CEB-FIB, CEB-FIP Model Code 1990 - Design Code, Thomas Telford, 1993.
- [48] Novak, L.C., Sprenger, H., Example 4: Deep Beam with opening, In: *ACI SP-208, Examples for the Design of Structural Concrete with Strut-and-tie Models*, Editor Karls-Heinz Reineck, ACI SP-208, 2002.


ORCID iD

Julian Alves Borges  <https://orcid.org/0000-0002-0986-7634>

Rodrigo Reis Amaral  <https://orcid.org/0000-0001-9035-5806>

Liércio André Isoldi  <https://orcid.org/0000-0002-9337-3169>

Walter Jesus Paucar Casas  <https://orcid.org/0000-0001-7712-2768>

Herbert Martins Gomes  <https://orcid.org/0000-0001-5635-1852>



© 2022 Shahid Chamran University of Ahvaz, Ahvaz, Iran. This article is an open-access article distributed under the terms and conditions of the Creative Commons Attribution-NonCommercial 4.0 International (CC BY-NC 4.0 license) (<http://creativecommons.org/licenses/by-nc/4.0/>).

How to cite this article: Borges J.A., Amaral R.R., Isoldi L.A., Casas W.J.P., Gomes H.M. A Novel BESO Methodology for Topology Optimization of Reinforced Concrete Structures: A Two-loop Approach, *J. Appl. Comput. Mech.*, 9(2), 2023, 498-512.
<https://doi.org/10.22055/jacm.2022.41708.3799>

Publisher's Note Shahid Chamran University of Ahvaz remains neutral with regard to jurisdictional claims in published maps and institutional affiliations.

